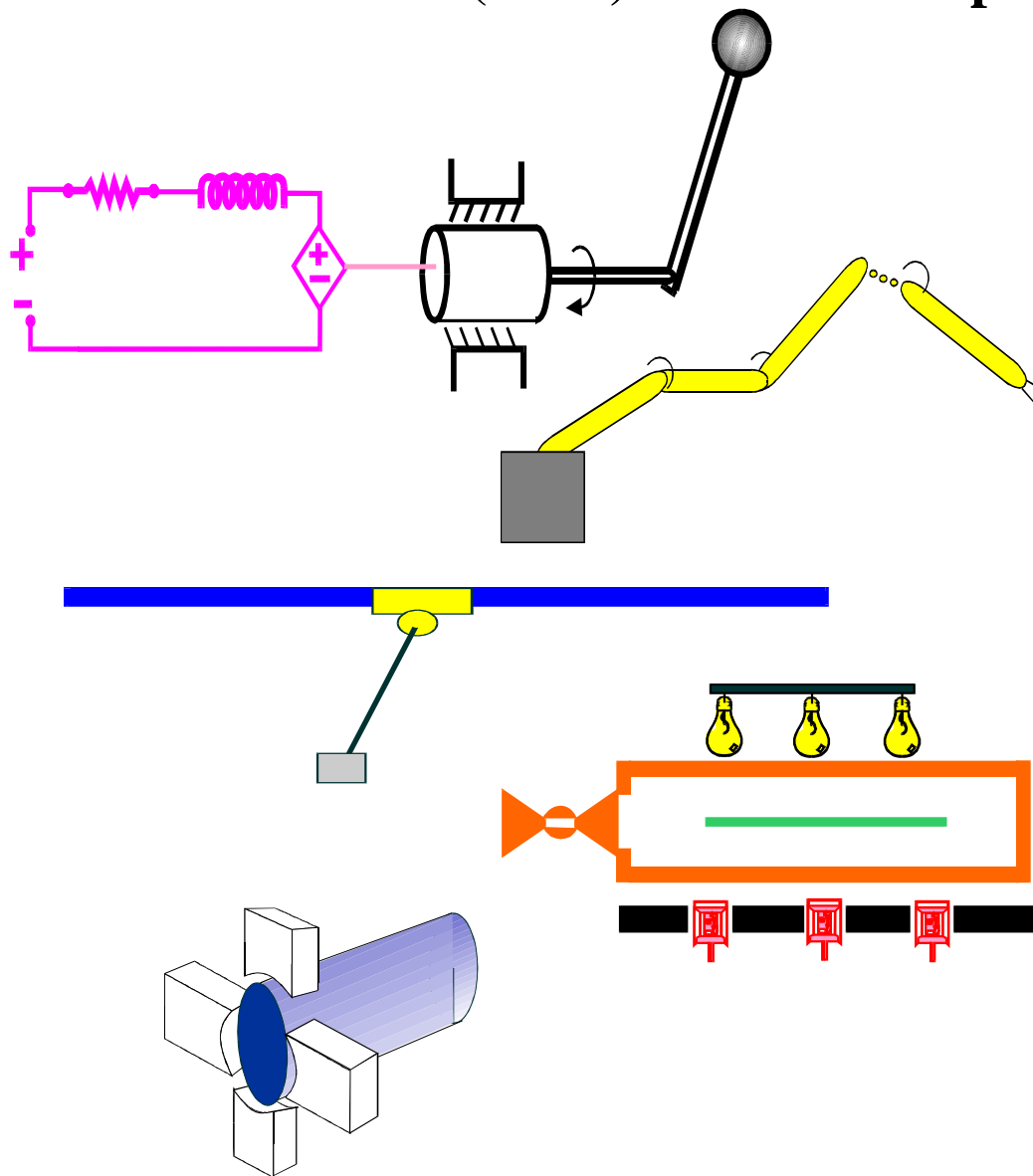


Clemson University
College of Engineering and Science
Control and Robotics (CRB) Technical Report



Number: CU/CRB/8/6/07/#1

Title: New Dynamic Models for Planar Extensible
Continuum Robot Manipulators

Authors: E. Tatlicioglu, I. D. Walker, and D. M. Dawson

New Dynamic Models for Planar Extensible Continuum Robot Manipulators

Enver Tatlicioglu*, Ian D. Walker, and Darren M. Dawson

Abstract: In this paper, the dynamic model for planar continuum manipulators that was presented in our previous work is extended to include new terms reflecting the effects of potential energy. First the gravitational potential energy of the manipulator is derived. Then, the elastic potential energy of the manipulator is derived for both bending and extension. Finally, the effects of the total potential energy are included in the dynamic model. Numerical simulation results are presented for a planar 3-section extensible continuum robot manipulator. The results show a much stronger match to physical continuum robots than with previously available models.

I. INTRODUCTION

The desire to enhance the performance and effectiveness of robot manipulators resulted in increasing interest in continuum robots [1]. To our best knowledge, the first design of continuum robots was introduced in the 1960's [2]. Numerous designs and prototypes of continuum robots were presented in [3], [4], [5], [6], and [7]. In the last two decades, there has been an increasing interest in designing and constructing 'biologically inspired' continuum robots. Most of these designs are inspired from trunks [8], [9], tentacles [10], [11], [12] and snakes [5]. Due to a wide variety of commercial applications, some implementations have appeared commercially (i.e., [13] and [14]).

The OCTARM (OCTOPUS ARM) in the Mechatronics Laboratory at Clemson University, which is a biologically inspired soft robot manipulator, resembles an elephant trunk or an octopus arm [15]. It is a three-section robot with nine degrees of freedom where each section has capability of extension along with two axis bending with constant curvature. Its design makes OCTARM suitable for a wide variety of applications ranging from whole arm grasping of various shapes of payloads to navigation of unstructured environments [10]. In [16], Walker *et al.* discussed the workspace of OCTARM for planar case and showed that it provides an increased workspace compared to its inextensible counterparts. In [17], Jones and Walker presented a kinematic model for a general class of continuum robots which has been applied to OCTARM. In a recent work, Jones and

Walker [18] discussed the limiting-case analysis for a general class of continuum manipulators. However, kinematic control of continuum robot hardware remains the state of the art due to the current lack of appropriate dynamic models.

There has been some previous research in dynamic modeling of biologically inspired robot manipulators [19], [20], [21], [22], [23], [24], [25], and [26]. In [19], [20], the authors presented dynamic models for snake-like robots where serial rigid-link systems are considered. In [21], Yekutieli *et al.* presented a 2-D dynamic model for an extensible octopus arm based on an approximation to the true continuum case. In [22], Chirikjian proposed a dynamic model for hyper-redundant robot manipulators based on an approximation to an infinite-degree-of-freedom continuum model. The papers presented by Ivanescu [23] and Mochiyama [24], [25], [26] considered dynamic modeling of continuum robot manipulators. The proposed dynamic model in [24] was for inextensible robot manipulators and did not include elastic potential energy terms due to bending effects. In the literature, the closest work to that in this paper was presented in [23]. Ivanescu *et al.* considered both gravitational and elastic potential energy effects when deriving their model. However, the elastic potential energy due to bending was calculated as a summation of all the elements of the manipulator and while deriving the elastic potential energy due to bending and extension the spring constants were considered to be the same along the backbone curve of the manipulator. This approach results in an approximation of the elastic potential energy and does not reflect the characteristics of different sections of the physical manipulators.

In this paper, the dynamic model for planar continuum manipulators that was presented in our previous work [27] is extended to include new terms due to the effects of the potential energy. The dynamic model in [27] was derived based on the assumption that the manipulator had no potential energy. While that approach is a reasonable assumption when starting the derivation of a novel dynamic model, the next required step is to include the effects of applicable potential energy. In order to do this, first, based on the definition presented in [24], the gravitational potential energy of one backbone slice is derived. After integrating the gravitational potential energy of one slice along the backbone curve the total gravitational potential energy of the robot manipulator is calculated. Then, the elastic potential energy of the manipulator is considered. First, the elastic potential energy due to the effects of bending is derived for one slice of the manipulator. After integrating the elastic potential energy of one slice along the backbone curve the total elastic potential energy due to bending is calculated. Next, elastic potential energy reflecting the ex-

This work is supported in part by a DOC Grant, an ARO Automotive Center Grant, a DOE Contract, a Honda Corporation Grant, and by the Defense Advanced Research Projects Agency (DARPA), Contract Number N66001-C-8043 and by the National Science Foundation under grant number IIS-0534423.

The authors are with the Department of Electrical & Computer Engineering, Clemson University, Clemson, SC 29634-0915. [etatlic,ianw,darren.dawson]@ces.clemson.edu.

* Corresponding author. Phone & Fax: 864-656-7218

tensibility of our model is considered. The elastic potential energy caused by extension is calculated by modeling each section of the manipulator as a spring. The total elastic potential energy of the manipulator due to extension effects is found by adding the corresponding energy terms of each section. While deriving the elastic potential energy, separate spring constants are assigned for each section of the robot manipulator to reflect the different characteristics of different sections of the physical manipulator. This approach provides an improvement over a similar definition introduced in [23] where the spring constant was assumed to be the same along the backbone curve. Finally, by utilizing Lagrangian representation the effects of the potential energy are reflected to the dynamic model that was presented in [27]. Numerical simulation results are presented for a planar 3-section extensible continuum robot manipulator.

II. SYSTEM MODEL

In this section, system model and properties are presented. For a more detailed analysis of the system model, the reader is referred to [27] or [28]. The geometric model of a 3-section extensible continuum robot manipulator utilized in this paper is presented in Figure 2. This geometric model is a good approximation of the OCTARM which is shown in Figure 1.

Similar to [27], the following convention, which is adopted from [24], will be adhered throughout the following development. The orientation matrix of the base frame and the position vector of the origin are represented by ${}^0\Phi(0) \in SO(3)$ and ${}^0p(0) \in \mathbb{R}^3$ respectively. The position vectors of the point σ relative to the origin as viewed from the base frame and ${}^\xi p(\xi, t)$ are denoted by ${}^0p(\sigma, t)$ and ${}^\xi p(\sigma, t) \in \mathbb{R}^3$, respectively. The curvature at the point σ is represented by $\kappa(\sigma, t) \in \mathbb{R}$ and section lengths of the robot manipulator are denoted as $d_i(t) \in \mathbb{R}_+$, $i = 1, 2, 3$. The total length of the robot manipulator, denoted as $d(t) \in \mathbb{R}_+$, is equal to the following

$$d(t) \triangleq d_1(t) + d_2(t) + d_3(t). \quad (1)$$

The system model is assumed to satisfy the following properties.

Property 1: The curvature κ at each point σ of the manipulator is a function of both time and σ . In the following analysis, consistent with the OCTARM, it is assumed that the curvature of a section is only function of time (i.e., $\kappa(\sigma, t) = \kappa_i(t)$ if σ is a point on Section i , $i = 1, 2, 3$). In the subsequent analysis, it is assumed that the curvature is always non-zero (i.e., $\kappa(\sigma, t) \neq 0 \forall (\sigma, t)$). The reader is referred to [18] for a detailed limiting-case analysis for a general class of continuum robot manipulators.

Property 2: In Figure 2, $p(\xi, t) \in \mathbb{R}^3$ is the position vector of point ξ of the backbone curve and $p_c(\xi, t) \in \mathbb{R}^3$ is the position vector of the center of mass of the slice at ξ . In the analysis, again consistent with the OCTARM, it is assumed that $p(\xi, t)$ and $p_c(\xi, t)$ coincide (i.e., $\Delta p(\xi) = [0 \ 0 \ 0]^T$).

Property 3: The robot manipulator is assumed to have uniform mass density. The line mass density of the slice, denoted as $m(\sigma, t) \in \mathbb{R}$, is defined as follows

$$m(\sigma, t) = \frac{m}{d(t)} \quad (2)$$

where $m \in \mathbb{R}$ is the total mass of the manipulator.

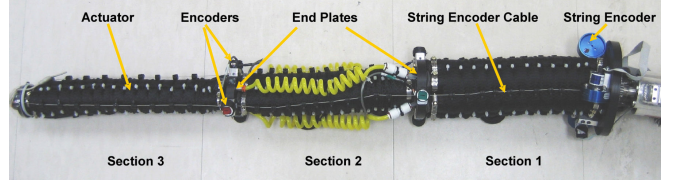


Fig. 1. OCTARM (ver. 5.2)

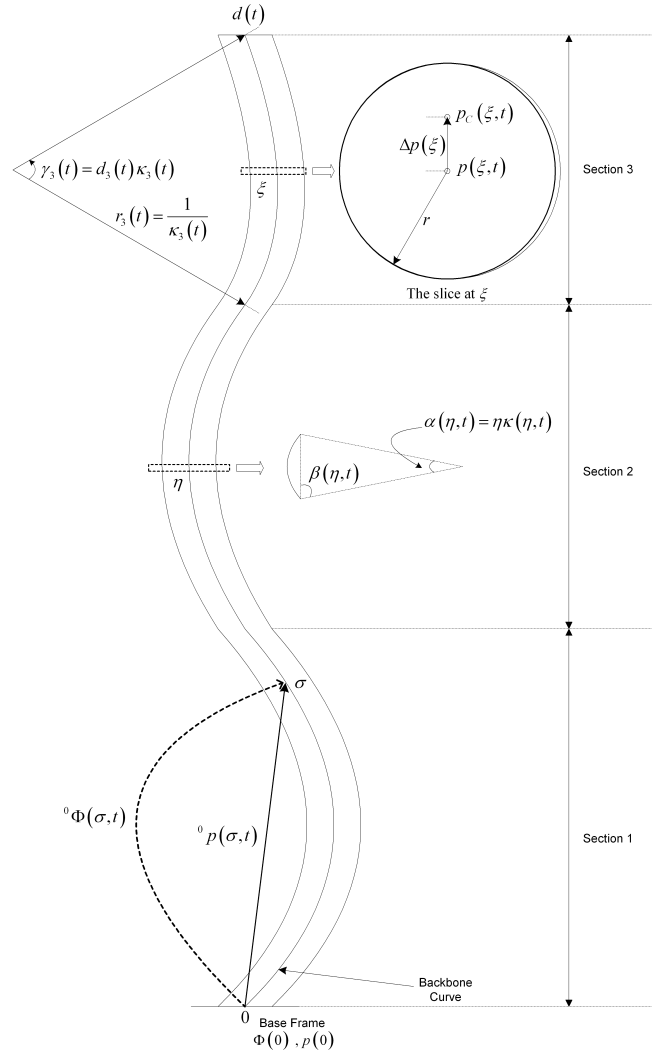


Fig. 2. Geometry of a 3-Section Extensible Robot Manipulator

The orientation matrix of the extended Frenet frame at σ with respect to the base frame, denoted as ${}^0\Phi(\sigma, t)$, is given

as follows [17]

$${}^0\Phi(\sigma, t) = \begin{bmatrix} \cos(\sigma\kappa(\sigma, t)) & 0 & -\sin(\sigma\kappa(\sigma, t)) \\ 0 & 1 & 0 \\ \sin(\sigma\kappa(\sigma, t)) & 0 & \cos(\sigma\kappa(\sigma, t)) \end{bmatrix}. \quad (3)$$

The position vector of any point σ from the origin with respect to the base frame, denoted as ${}^0p(\sigma, t)$, is evaluated as follows

$${}^0p(\sigma, t) = \int_0^\sigma {}^0\Phi(\eta, t) e_\times d\eta \quad (4)$$

where $e_\times \triangleq [1 \ 0 \ 0]^T$.

III. POTENTIAL ENERGY

In this section, three different energy definitions will be introduced for our model. First, gravitational potential energy will be defined and then the elastic potential energy due to both bending and extension will be presented.

A. Gravitational Potential Energy

The gravitational potential energy of a slice at σ is given as follows [24]

$$P_g(\sigma, t) \triangleq -m(\sigma, t) \sigma g^T(\sigma, t) p(\sigma, t) \quad (5)$$

where $\sigma g^T(\sigma, t) \in \mathbb{R}^3$ is defined as follows

$$\sigma g^T(\sigma, t) \triangleq \sigma \Phi^T(0, t) [0 \ 0 \ -g]^T \quad (6)$$

where $g \in \mathbb{R}$ is the gravity acceleration constant. After utilizing (2), (4), (6) gravitational potential energy can be calculated as follows

$$P_g(\sigma, t) = \frac{mg}{d(t)\kappa(\sigma, t)} [\cos(\sigma\kappa(\sigma, t)) - \cos(2\sigma\kappa(\sigma, t))]. \quad (7)$$

Total gravitational potential energy of the system can be found as a sum of the gravitational energies for every slice

$$P_g(t) \triangleq \int_0^{d(t)} P_g(\sigma, t) d\sigma \quad (8)$$

where $P_g(\sigma, t)$ is the gravitational potential energy of the slice at σ defined in (5) and (7). It should be noted that, the upper limit of the integral in (8) is the total length of the manipulator, which is a function of time as a result of the extensible nature of our geometric model, while the total length of the manipulator in [24] was constant. To facilitate the subsequent development, the total gravitational potential energy of the system will be rewritten as follows¹

$$P_g(t) = \int_0^{d_1} P_{g1}(\sigma, t) d\sigma + \int_{d_1}^{d_1+d_2} P_{g2}(\sigma, t) d\sigma + \int_{d_1+d_2}^{d_1+d_2+d_3} P_{g3}(\sigma, t) d\sigma \quad (9)$$

¹For simplicity, the time dependency of the section lengths in (9) is dropped.

where $P_{gi}(\sigma, t)$ is the gravitational potential energy of slice σ when σ is a point on Section i , $i = 1, 2, 3$ which is defined as follows

$$P_{gi}(\sigma, t) = \frac{mg}{d\kappa_i} [\cos(\sigma\kappa_i) - \cos(2\sigma\kappa_i)]. \quad (10)$$

From (9) $P_g(t)$ can be calculated as follows

$$P_g = \frac{mg}{d} \left\{ \frac{1}{\kappa_1^2} \left[\sin(d_1\kappa_1) - \frac{1}{2} \sin(2d_1\kappa_1) \right] + \frac{1}{\kappa_2^2} \left[\sin((d_1+d_2)\kappa_2) - \frac{1}{2} \sin(2(d_1+d_2)\kappa_2) - \sin(d_1\kappa_2) + \frac{1}{2} \sin(2d_1\kappa_2) \right] + \frac{1}{\kappa_3^2} \left[\sin((d_1+d_2+d_3)\kappa_3) - \frac{1}{2} \sin(2(d_1+d_2+d_3)\kappa_3) - \sin((d_1+d_2)\kappa_3) + \frac{1}{2} \sin(2(d_1+d_2)\kappa_3) \right] \right\} \quad (11)$$

where (10) was utilized.

B. Elastic Potential Energy

In this section, potential energy due to extension and bending is discussed.

1) *Elastic Potential Energy due to Bending*: The elastic potential energy of the manipulator due to bending is given as follows

$$P_b(t) \triangleq \frac{1}{2} \int_0^{d(t)} k_b(\sigma) \beta^2(\sigma, t) d\sigma. \quad (12)$$

In (12), $\beta(\sigma, t)$ is defined as follows

$$\beta(\sigma, t) \triangleq \pi - \frac{1}{2} \alpha(\sigma, t) \quad (13)$$

where $\alpha(\sigma, t)$ is defined as follows

$$\alpha(\sigma, t) \triangleq \sigma\kappa(\sigma, t) \quad (14)$$

and $k_b(\sigma)$ is the spring constant defined as follows

$$k_b(\sigma) \triangleq k_{bi} \text{ if } \sigma \text{ is a point on Section } i, i=1,2,3. \quad (15)$$

This definition of the spring constants allows us to define different spring constants for each section. This definition of the elastic potential energy due to bending provides an improvement over a similar definition introduced in [23]. In [23], the potential energy is in the form of a summation as opposed to the integral form presented in this paper, and also the spring constant utilized in that derivation is constant for the manipulator. The total elastic potential energy due to bending can be written as follows

$$P_b(t) = \frac{1}{2} k_{b1} \int_0^{d_1} \beta_1^2(\sigma, t) d\sigma + \frac{1}{2} k_{b2} \int_{d_1}^{d_1+d_2} \beta_2^2(\sigma, t) d\sigma + \frac{1}{2} k_{b3} \int_{d_1+d_2}^{d_1+d_2+d_3} \beta_3^2(\sigma, t) d\sigma \quad (16)$$

where (15) was utilized, and from (13) and (14), $\beta_i(\sigma, t)$, $i = 1, 2, 3$ can be defined as follows

$$\beta_i(\sigma, t) \triangleq \pi - \frac{1}{2}\sigma\kappa_i. \quad (17)$$

The total elastic potential energy due to bending evaluated in closed-form is presented as follows

$$\begin{aligned} P_b = & \frac{1}{2}k_{b1} \left[\pi^2 d_1 - \frac{1}{2}\pi d_1^2 \kappa_1 + \frac{1}{12}\pi d_1^3 \kappa_1^2 \right] \\ & + \frac{1}{2}k_{b2} \left\{ \left[\pi^2 (d_1 + d_2) - \frac{1}{2}\pi (d_1 + d_2)^2 \kappa_2 \right. \right. \\ & \left. \left. + \frac{1}{12}\pi (d_1 + d_2)^3 \kappa_2^2 \right] \right. \\ & \left. - \left[\pi^2 d_1 - \frac{1}{2}\pi d_1^2 \kappa_2 + \frac{1}{12}\pi d_1^3 \kappa_2^2 \right] \right\} \\ & + \frac{1}{2}k_{b3} \left\{ \left[\pi^2 (d_1 + d_2 + d_3) \right. \right. \\ & \left. \left. - \frac{1}{2}\pi (d_1 + d_2 + d_3)^2 \kappa_3 \right. \right. \\ & \left. \left. + \frac{1}{12}\pi (d_1 + d_2 + d_3)^3 \kappa_3^2 \right] \right. \\ & \left. - \left[\pi^2 (d_1 + d_2) - \frac{1}{2}\pi (d_1 + d_2)^2 \kappa_3 \right. \right. \\ & \left. \left. + \frac{1}{12}\pi (d_1 + d_2)^3 \kappa_3^2 \right] \right\}. \quad (18) \end{aligned}$$

2) *Elastic Potential Energy due to Extension:* The elastic potential energy of the manipulator due to extension is given as follows

$$\begin{aligned} P_e \triangleq & \frac{1}{2}k_{e1} [d_1(t) - d_1^*]^2 + \frac{1}{2}k_{e2} [d_2(t) - d_2^*]^2 \\ & + \frac{1}{2}k_{e3} [d_3(t) - d_3^*]^2 \quad (19) \end{aligned}$$

where d_i^* is the constant relaxed length of the i^{th} section and k_{ei} are spring constants for each section of the manipulator. This definition of the spring constants provides an improvement on the model in [23] which utilized the same spring constant for that definition.

IV. LAGRANGIAN REPRESENTATION

Since the derivation in [27] was based on the assumption that the system had no potential energy, the Lagrangian was defined as

$$L(t) = K(t) \quad (20)$$

where $K(t)$ represents the total kinetic energy of the system. Based on the following Euler-Lagrange equations of motion [29]

$$\frac{d}{dt} \frac{\partial L}{\partial \dot{q}_i} - \frac{\partial L}{\partial q_i} = \tau_i, \quad i = 1, 2, \dots, 6. \quad (21)$$

the dynamic model of the system in [27] and [28] was developed as

$$M(q) \ddot{q} + V(q, \dot{q}) \dot{q} = \tau(t) \quad (22)$$

where $M(q)$, $V(q, \dot{q}) \in \mathbb{R}^{6 \times 6}$ are inertia matrix and centripetal-coriolis terms, respectively, $\tau(t) \in \mathbb{R}^6$ is the

control input, and $q(t) \in \mathbb{R}^6$ is the joint position vector defined as follows

$$q \triangleq [d_1 \quad d_2 \quad d_3 \quad \kappa_1 \quad \kappa_2 \quad \kappa_3]^T. \quad (23)$$

Due to space constraints, the entries of the inertia matrix $M(q)$ and the centripetal-coriolis terms $V(q, \dot{q})$ were presented in [28]. Since in this derivation we assume the existence of potential energy, the Lagrangian of the new system is defined as follows

$$L(t) \triangleq K(t) - P(t) \quad (24)$$

where $P(t)$ represents the total potential energy of the system defined as follows

$$P(t) \triangleq P_g(t) + P_b(t) + P_e(t) \quad (25)$$

where $P_g(t)$ is the gravitational potential energy, and $P_b(t)$ and $P_e(t)$ represent elastic potential energy due to extension and bending, respectively. It is easy to see that the potential energy terms $P_g(t)$, $P_b(t)$ and $P_e(t)$, defined in (11), (18), (19) respectively, are functions of only joint position vector $q(t)$ (i.e., they are not functions of the joint velocities or accelerations). The Lagrangian can be rewritten as follows

$$\frac{d}{dt} \frac{\partial K}{\partial \dot{q}_i} - \frac{\partial K}{\partial q_i} - \frac{d}{dt} \frac{\partial P}{\partial \dot{q}_i} + \frac{\partial P}{\partial q_i} = \tau_i, \quad i = 1, 2, \dots, 6. \quad (26)$$

where (24) was utilized. The first two terms on the left-hand-side of (26) were calculated in [28]. Since the total potential energy of the system is not a function of the joint velocities, then it is clear that the third term on the left-hand-side of (26) is equal to zero for $\forall i$. The final term on the left-hand-side of (26) can be written as follows

$$\frac{\partial P}{\partial q_i} = \frac{\partial P_g}{\partial q_i} + \frac{\partial P_b}{\partial q_i} + \frac{\partial P_e}{\partial q_i}, \quad i = 1, 2, \dots, 6. \quad (27)$$

In view of the above mentioned facts, the dynamic model of the system is developed as follows

$$M(q) \ddot{q} + V(q, \dot{q}) \dot{q} + G(q) + B(q) + E(q) = \tau(t) \quad (28)$$

where $G(q)$, $B(q)$, $E(q) \in \mathbb{R}^6$ represent the effects of $P_g(t)$, $P_b(t)$, and $P_e(t)$ respectively, which are defined as follows

$$G = [G_1 \quad G_2 \quad G_3 \quad G_4 \quad G_5 \quad G_6]^T, \quad (29)$$

$$B = [B_1 \quad B_2 \quad B_3 \quad B_4 \quad B_5 \quad B_6]^T, \quad (30)$$

$$E = [E_1 \quad E_2 \quad E_3 \quad E_4 \quad E_5 \quad E_6]^T \quad (31)$$

where the individual entries are defined as follows

$$G_i \triangleq \frac{\partial P_g}{\partial q_i} \quad B_i \triangleq \frac{\partial P_b}{\partial q_i} \quad E_i \triangleq \frac{\partial P_e}{\partial q_i}. \quad (32)$$

The terms $G_i(q)$, $B_i(q)$, $E_i(q) \forall i, i = 1, \dots, 6$ are defined in Appendix I.

V. NUMERICAL RESULTS

To underline the validity of the proposed dynamic model, two numerical simulations are performed. The model is implemented in Matlab 7.0.

A. First Simulation Run

In the first simulation run, to illustrate the similarities to the physical system, the system is fed with $\tau_6(t)$ being a sinusoid with an amplitude of 10^{-4} [Nm] and a period of 10 [sec] where the other entries of the control input $\tau(t)$ set to zero. The spring constants are chosen as

$$k_{bi} = 0.001, k_{ei} = 10, \forall i = 1, 2, 3. \quad (33)$$

The section lengths and the curvatures² are presented in Figures 3 and 4, respectively. While the changes in the section lengths are negligible (i.e., less than 5mm for each section), the effects observed on the curvatures are decreasing from $\kappa_3, \kappa_2, \kappa_1$ as expected from a real physical system.

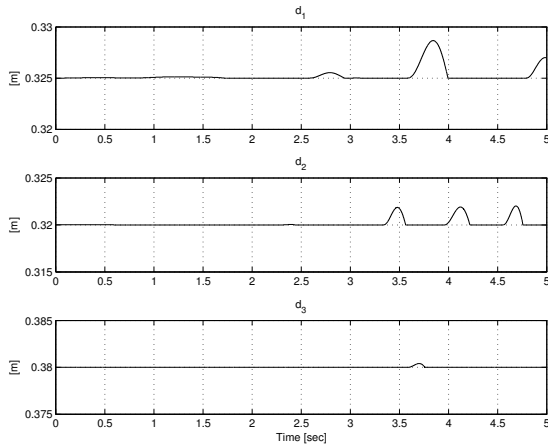


Fig. 3. The section lengths for the first simulation

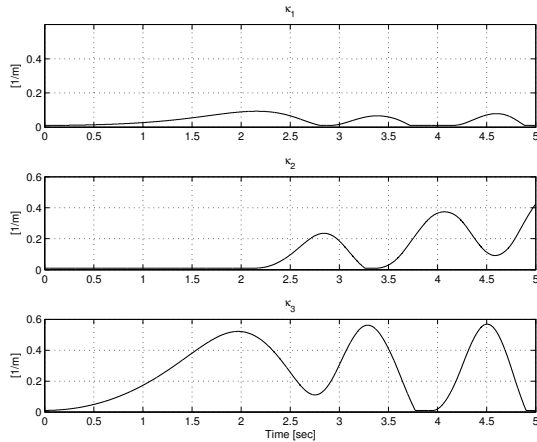


Fig. 4. The curvatures for the first simulation

²As previously discussed in Property 1, manipulator curvatures are non-zero. Based on this, the initial curvature values on both simulations are set to be equal to 0.01 [1/m] to show the performance of the manipulator near its limits.

B. Second Simulation Run

In the second simulation run, a straightforward control scheme for robot manipulators, namely a computed-torque controller is implemented. The tracking error signal $e(t) \in \mathbb{R}^6$ is defined as follows

$$e \triangleq q_d - q \quad (34)$$

where $q_d(t) \in \mathbb{R}^6$ is the desired joint positions. The dynamic model presented in (28) is rewritten as follows

$$M(q)\ddot{q} + N(q, \dot{q}) = \tau(t) \quad (35)$$

where $N(q, \dot{q}) \in \mathbb{R}^6$ represents the other dynamic effects on the left-hand-side of (28). The control input $\tau(t)$ is designed as follows [30]

$$\tau \triangleq M(\ddot{q}_d + K_v\dot{e} + K_p e) + N \quad (36)$$

where $K_v, K_p \in \mathbb{R}^{6 \times 6}$ are constant control gain matrices. Since it is not in the scope of this paper, the stability analysis for the suggested controller is omitted and the reader is referred to Section 4.4 of [30] for a more detailed analysis.

To show the tracking performance of the proposed dynamic model $q_d(t)$ is selected as follows

$$q_d = \begin{bmatrix} 0.35 + 0.01 \sin(2\pi t) \\ 0.35 \\ 0.40 + 0.01 \sin(2\pi t) \\ 1 + 0.2 \sin(2\pi t) \\ 2 + 0.2 \sin(2\pi t) \\ 3 \end{bmatrix}. \quad (37)$$

The control gains are chosen as follows

$$K_v = I_6, K_p = 100I_6 \quad (38)$$

where $I_6 \in \mathbb{R}^{6 \times 6}$ is the standard identity matrix. The spring constants defined in (33) are utilized. In Figures 5 and 6, the section lengths and the curvatures² are presented, respectively. In Figures 7 and 8, the tracking error signals for the section lengths and the curvatures are presented, respectively. From Figures 7 and 8, it is clear that the tracking error signals are driven to zero. The control inputs are presented in Figures 9 and 10.

VI. CONCLUSIONS

The dynamic model for planar continuum robot manipulators presented in [27] was extended to include new terms to reflect the effects of gravitational and elastic potential energy. In order to do this, first, the total gravitational potential energy of the robot manipulator is calculated. Then, the elastic potential energy terms due to bending and extension effects were derived. Finally, the effects of the total potential energy were reflected to the dynamic model in [27] by utilizing the Lagrangian representation. It should be noted that since the new terms introduced in the dynamic model are functions of only the joint position vector then the dynamic model satisfies the skew-symmetric property as shown in [27]. Numerical simulation results are presented for a planar 3-section extensible continuum robot manipulator.

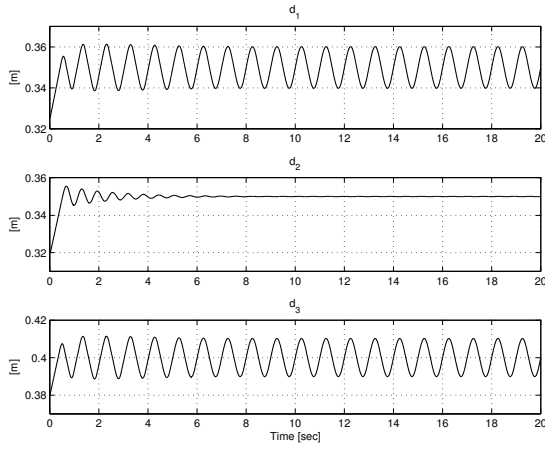


Fig. 5. The section lengths for the second simulation

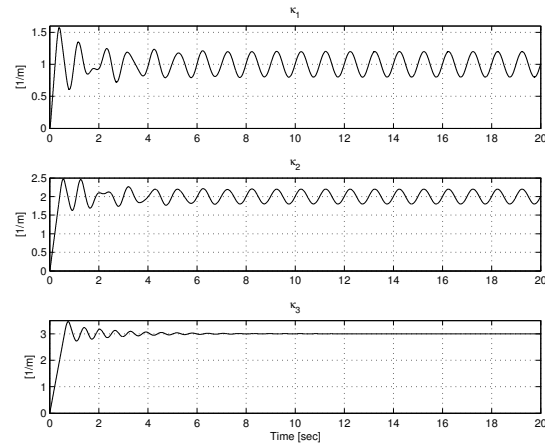


Fig. 6. The curvatures for the second simulation

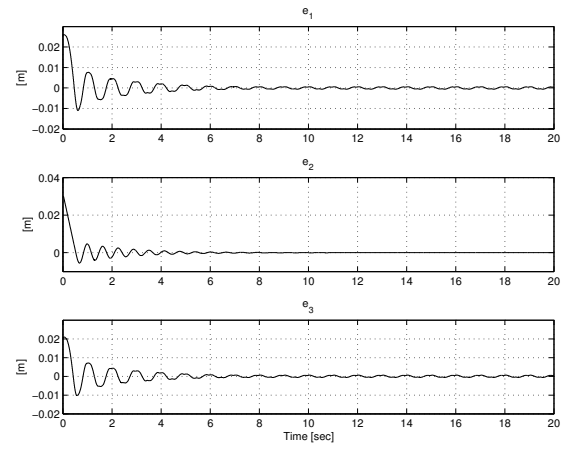


Fig. 7. The tracking error for the section lengths for the second simulation

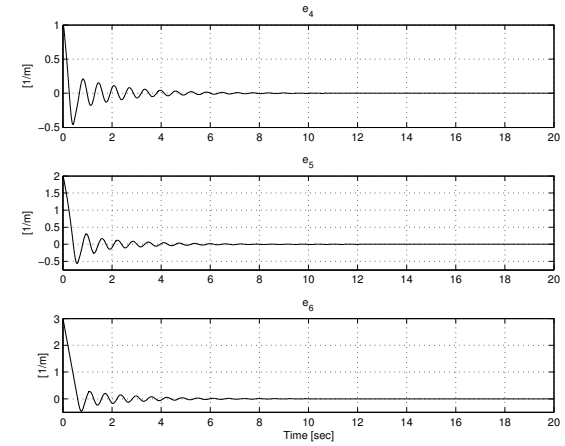


Fig. 8. The tracking error for the curvatures for the second simulation

The results show good consistency with the behavior of continuum robot hardware, and good potential for use in controller implementation.

REFERENCES

- [1] G. Robinson and J. Davies, "Continuum robots - a state of the art," in *Proc. IEEE Int. Conf. Robot. Autom.*, Detroit, MI, 1999, pp. 2849–2854.
- [2] V. Anderson and R. Horn, "Tensor arm manipulator design," *Transactions of the ASME*, vol. 67-DE-57, pp. 1–12, 1967.
- [3] G. Chen, P. Tu, T. Herve, and C. Prellle, "Design and modeling of a micro-robotic manipulator for colonoscopy," in *Proc. of the 41st SICE Annual Conference*, Annecy, France, 2005, pp. 109–114.
- [4] G. Chirikjian and J. Burdick, "A hyper-redundant manipulator," *IEEE Robot. Automat. Mag.*, vol. 1, no. 4, pp. 22–29, 1994.
- [5] S. Hirose, *Biologically Inspired Robots*. New York, NY: Oxford University Press, 1993.
- [6] M. Ivanescu and V. Stoian, "A variable structure controller for a tentacle manipulator," in *Proc. IEEE Int. Conf. Robot. Autom.*, Nagoya, Japan, 1995, pp. 3155–3160.
- [7] D. Lane, J. Davies, G. Robinson, D. O'Brien, J. Sneddon, E. Seaton, and A. Elfstrom, "The amadeus dextrous subsea hand: Design, modeling, and sensor processing," *IEEE J. Oceanic Eng.*, vol. 24, no. 1, pp. 96–111, 1999.
- [8] R. Cieslak and A. Morecki, "Elephant trunk type elastic manipulator a tool for bulk and liquid type materials transportation," *Robotica*, vol. 17, no. 1, pp. 11–16, 1999.
- [9] H. Tsukagoshi, A. Kitagawa, and M. Segawa, "Active hose: An artificial elephant's nose with maneuverability for rescue operation," in *Proc. IEEE Int. Conf. Robot. Autom.*, Seoul, Korea, 2001, pp. 2454–2459.
- [10] W. McMahan, B. Jones, V. Chitrakaran, M. Csencsits, M. Grissom, M. Pritts, C. Rahn, and I. Walker, "Field trials and testing of the octarm continuum manipulator," in *Proc. IEEE Int. Conf. Robot. Autom.*, Orlando, FL, 2006, pp. 2336–2341.
- [11] H. Ohno and S. Hirose, "Design of slim slime robot and its gait of locomotion," in *Proc. IEEE/RSJ Int. Conf. Intell. Robots Syst.*, Maui, HI, 2001, pp. 707–715.
- [12] K. Suzumori, S. Iikura, and H. Tanaka, "Development of flexible microactuator and its applications to robotic mechanisms," in *Proc. IEEE Int. Conf. Robot. Autom.*, Sacramento, CA, 1991, pp. 1622–1627.
- [13] R. Buckingham and A. Graham, "Snaking around in a nuclear jungle," *Industrial Robot: An International Journal*, vol. 32, no. 2, pp. 120–127, 2005.
- [14] G. Immega and K. Antonelli, "The ksi tentacle manipulator," in *Proc. IEEE Int. Conf. Robot. Autom.*, Nagoya, Japan, 1995, pp. 3149–3154.
- [15] W. McMahan, B. Jones, and I. Walker, "Robotic manipulators inspired by cephalopod limbs," *J. Engineering Design and Innovation*, vol. 1P-01P2, 2005.
- [16] I. Walker, C. Carreras, R. McDonnell, and G. Grimes, "Extension

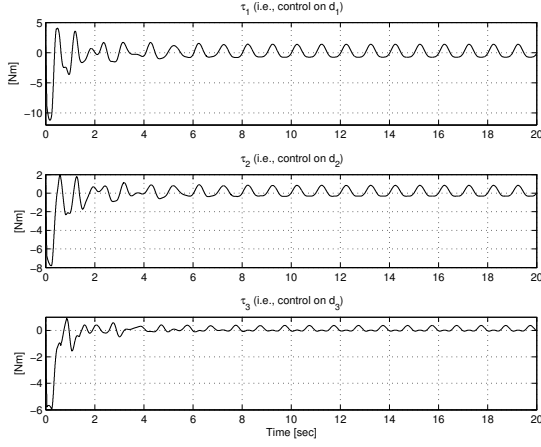


Fig. 9. The control inputs for section lengths (i.e., $\tau_1(t)$, $\tau_2(t)$, and $\tau_3(t)$) for the second simulation

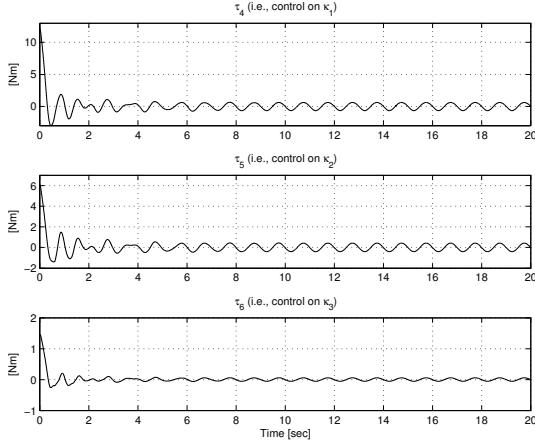


Fig. 10. The control inputs for curvatures (i.e., $\tau_4(t)$, $\tau_5(t)$, and $\tau_6(t)$) for the second simulation

versus bending for continuum robots,” *Intl. J. Advanced Robotic Systems*, vol. 3, no. 2, pp. 171–178, 2006.

- [17] B. Jones and I. Walker, “Kinematics for multi-section continuum robots,” *IEEE Transactions on Robotics*, vol. 22, no. 1, pp. 43–55, 2006.
- [18] —, “Limiting-case analysis of continuum trunk kinematics,” in *Proc. IEEE Int. Conf. Robot. Autom.*, Rome, Italy, 2007, pp. 1363–1368.
- [19] W. Khalil, G. Gallot, O. Ibrahim, and F. Boyer, “Dynamic modeling of a 3-d serial eel-like robot,” in *Proc. IEEE Int. Conf. Robot. Autom.*, Barcelona, Spain, 2005, pp. 1282–1287.
- [20] F. Matsuno and H. Sato, “Trajectory tracking control of snake robots based on dynamic model,” in *Proc. IEEE Int. Conf. Robot. Autom.*, Barcelona, Spain, 2005, pp. 3040–3045.
- [21] Y. Yekutieli, R. Sagiv-Zohar, R. Aharonov, Y. Engel, B. Hochner, and T. Flash, “Dynamic model of the octopus arm. i. biomechanics of the octopus arm reaching movement,” *Journal of Neurophysiology*, vol. 94, pp. 1443–1458, 2005.
- [22] G. Chirikjian, “Hyper-redundant manipulator dynamics: A continuum approximation,” *Advanced Robotics*, vol. 9, no. 3, pp. 217–243, 1995.
- [23] M. Ivanescu, N. Popescu, and D. Popescu, “A variable length tentacle manipulator control system,” in *Proc. IEEE Int. Conf. Robot. Autom.*, Barcelona, Spain, 2005, pp. 3274–3279.
- [24] H. Mochiyama and T. Suzuki, “Dynamics modelling of a hyper-flexible manipulator,” in *Proc. of the 41st SICE Annual Conference*, Osaka, Japan, 2002, pp. 1505–1510.
- [25] H. Mochiyama, “Hyper-flexible robotic manipulators,” in *Proc. IEEE*

Int. Symposium on Micro-NanoMechatronics and Human Science, Nagoya, Japan, 2005, pp. 41–46.

- [26] H. Mochiyama and T. Suzuki, “Kinematics and dynamics of a cable-like hyper-flexible manipulator,” in *Proc. IEEE Int. Conf. Robot. Autom.*, Taipei, Taiwan, 2003, pp. 3672–3677.
- [27] E. Tatlicioglu, I. Walker, and D. Dawson, “Dynamic modeling for planar extensible continuum robot manipulators,” in *Proc. IEEE Int. Conf. Robot. Autom.*, Rome, Italy, 2007, pp. 1357–1362.
- [28] —, “Dynamic modelling for planar extensible continuum robot manipulators,” Clemson University CRB, Tech. Rep. CU/CRB/9/15/06/1, Sept. 2006. [Online]. Available: <http://www.ces.clemson.edu/ece/crb/publicn/tr.htm>
- [29] M. W. Spong and M. Vidyasagar, *Robot Dynamics and Control*. New York, NY: John Wiley and Sons, Inc., 1989.
- [30] F. Lewis, D. Dawson, and C. Abdallah, *Robot Manipulator Control: Theory and Practice*. New York, NY: Marcel Dekker, Inc., 2004.

APPENDIX I THE ENTRIES OF $G(q)$, $B(q)$, AND $E(q)$

A. Gravitational Terms

The entries of $G(q)$ are given as follows

$$\begin{aligned}
 G_1 \triangleq & \frac{mg}{d} \left\{ \frac{1}{\kappa_1} [\cos(d_1\kappa_1) - \cos(2d_1\kappa_1)] \right. & (39) \\
 & + \frac{1}{\kappa_2} [\cos((d_1+d_2)\kappa_2) - \cos(2(d_1+d_2)\kappa_2) \\
 & - \cos(d_1\kappa_2) + \cos(2d_1\kappa_2)] \\
 & + \frac{1}{\kappa_3} [\cos((d_1+d_2+d_3)\kappa_3) \\
 & - \cos(2(d_1+d_2+d_3)\kappa_3) \\
 & - \cos((d_1+d_2)\kappa_3) + \cos(2(d_1+d_2)\kappa_3)] \left. \right\} \\
 & - \frac{mg}{d^2} \left\{ \frac{1}{\kappa_1^2} \left[\sin(d_1\kappa_1) - \frac{1}{2} \sin(2d_1\kappa_1) \right] \right. \\
 & + \frac{1}{\kappa_2^2} \left[\sin((d_1+d_2)\kappa_2) - \frac{1}{2} \sin(2(d_1+d_2)\kappa_2) \right. \\
 & \left. \left. - \sin(d_1\kappa_2) + \frac{1}{2} \sin(2d_1\kappa_2) \right] \right. \\
 & + \frac{1}{\kappa_3^2} [\sin((d_1+d_2+d_3)\kappa_3) \\
 & - \frac{1}{2} \sin(2(d_1+d_2+d_3)\kappa_3) \\
 & \left. \left. - \sin((d_1+d_2)\kappa_3) + \frac{1}{2} \sin(2(d_1+d_2)\kappa_3) \right] \right\}
 \end{aligned}$$

$$\begin{aligned}
G_2 \triangleq & \frac{mg}{d} \left\{ \frac{1}{\kappa_2} [\cos((d_1 + d_2) \kappa_2) \right. \\
& - \cos(2(d_1 + d_2) \kappa_2) \\
& + \frac{1}{\kappa_3} [\cos((d_1 + d_2 + d_3) \kappa_3) \\
& - \cos(2(d_1 + d_2 + d_3) \kappa_3) \\
& - \cos((d_1 + d_2) \kappa_3) + \cos(2(d_1 + d_2) \kappa_3)] \\
& - \frac{mg}{d^2} \left\{ \frac{1}{\kappa_1^2} \left[\sin(d_1 \kappa_1) - \frac{1}{2} \sin(2d_1 \kappa_1) \right] \right. \\
& + \frac{1}{\kappa_2^2} \left[\sin((d_1 + d_2) \kappa_2) - \frac{1}{2} \sin(2(d_1 + d_2) \kappa_2) \right. \\
& \left. \left. - \sin(d_1 \kappa_2) + \frac{1}{2} \sin(2d_1 \kappa_2) \right] \right. \\
& + \frac{1}{\kappa_3^2} [\sin((d_1 + d_2 + d_3) \kappa_3) \\
& - \frac{1}{2} \sin(2(d_1 + d_2 + d_3) \kappa_3) \\
& \left. \left. - \sin((d_1 + d_2) \kappa_3) + \frac{1}{2} \sin(2(d_1 + d_2) \kappa_3) \right] \right\} \quad (40)
\end{aligned}$$

$$\begin{aligned}
G_3 \triangleq & \frac{mg}{d} \frac{1}{\kappa_3} [\cos((d_1 + d_2 + d_3) \kappa_3) \\
& - \cos(2(d_1 + d_2 + d_3) \kappa_3)] \\
& - \frac{mg}{d^2} \left\{ \frac{1}{\kappa_1^2} \left[\sin(d_1 \kappa_1) - \frac{1}{2} \sin(2d_1 \kappa_1) \right] \right. \\
& + \frac{1}{\kappa_2^2} \left[\sin((d_1 + d_2) \kappa_2) - \frac{1}{2} \sin(2(d_1 + d_2) \kappa_2) \right. \\
& \left. - \sin(d_1 \kappa_2) + \frac{1}{2} \sin(2d_1 \kappa_2) \right] \\
& + \frac{1}{\kappa_3^2} [\sin((d_1 + d_2 + d_3) \kappa_3) \\
& - \frac{1}{2} \sin(2(d_1 + d_2 + d_3) \kappa_3) \\
& \left. \left. - \sin((d_1 + d_2) \kappa_3) + \frac{1}{2} \sin(2(d_1 + d_2) \kappa_3) \right] \right\} \quad (41)
\end{aligned}$$

$$\begin{aligned}
G_4 \triangleq & -\frac{2mg}{d\kappa_1^3} \left[\sin(d_1 \kappa_1) - \frac{1}{2} \sin(2d_1 \kappa_1) \right] \\
& + \frac{mgd_1}{\kappa_1^2} [\cos(d_1 \kappa_1) - \sin(2d_1 \kappa_1)] \quad (42)
\end{aligned}$$

$$\begin{aligned}
G_5 \triangleq & -\frac{2mg}{d\kappa_2^3} \left[\sin((d_1 + d_2) \kappa_2) - \frac{1}{2} \sin(2(d_1 + d_2) \kappa_2) \right. \\
& \left. - \sin(d_1 \kappa_2) + \frac{1}{2} \sin(2d_1 \kappa_2) \right] \\
& + \frac{mg}{d\kappa_2^2} \{ (d_1 + d_2) [\cos((d_1 + d_2) \kappa_2) \\
& - \cos(2(d_1 + d_2) \kappa_2)] \\
& - d_1 [\cos(d_1 \kappa_2) - \cos(2d_1 \kappa_2)] \} \quad (43)
\end{aligned}$$

$$\begin{aligned}
G_6 \triangleq & -\frac{2mg}{d\kappa_3^3} [\sin((d_1 + d_2 + d_3) \kappa_3) \\
& - \frac{1}{2} \sin(2(d_1 + d_2 + d_3) \kappa_3) \\
& - \sin((d_1 + d_2) \kappa_3) + \frac{1}{2} \sin(2(d_1 + d_2) \kappa_3)] \\
& + \frac{mg}{d\kappa_3^2} \{ (d_1 + d_2 + d_3) [\cos((d_1 + d_2 + d_3) \kappa_3) \\
& - \cos(2(d_1 + d_2 + d_3) \kappa_3)] \\
& - (d_1 + d_2) [\cos((d_1 + d_2) \kappa_3) \\
& - \cos(2(d_1 + d_2) \kappa_3)] \} \quad (44)
\end{aligned}$$

B. Bending Terms

The entries of $B(q)$ are given as follows

$$\begin{aligned}
B_1 = & \frac{1}{2} k_{b1} \left(\pi - \frac{1}{2} d_1 \kappa_1 \right)^2 \\
& + \frac{1}{2} k_{b2} \left\{ \left(\pi - \frac{1}{2} (d_1 + d_2) \kappa_2 \right)^2 \right. \\
& \left. - \left(\pi - \frac{1}{2} d_1 \kappa_2 \right)^2 \right\} \\
& + \frac{1}{2} k_{b3} \left\{ \left(\pi - \frac{1}{2} (d_1 + d_2 + d_3) \kappa_3 \right)^2 \right. \\
& \left. - \left(\pi - \frac{1}{2} (d_1 + d_2) \kappa_3 \right)^2 \right\} \quad (45)
\end{aligned}$$

$$\begin{aligned}
B_2 = & \frac{1}{2} k_{b2} \left(\pi - \frac{1}{2} (d_1 + d_2) \kappa_2 \right)^2 \\
& + \frac{1}{2} k_{b3} \left\{ \left(\pi - \frac{1}{2} (d_1 + d_2 + d_3) \kappa_3 \right)^2 \right. \\
& \left. - \left(\pi - \frac{1}{2} (d_1 + d_2) \kappa_3 \right)^2 \right\} \quad (46)
\end{aligned}$$

$$B_3 = \frac{1}{2} k_{b3} \left(\pi - \frac{1}{2} (d_1 + d_2 + d_3) \kappa_3 \right)^2 \quad (47)$$

$$B_4(t) = \frac{1}{2} k_{b1} \left[-\frac{1}{2} \pi d_1^2 + \frac{1}{6} \pi d_1^3 \kappa_1 \right] \quad (48)$$

$$\begin{aligned}
B_5(t) = & \frac{1}{2} k_{b2} \left\{ \left[-\frac{1}{2} \pi (d_1 + d_2)^2 + \frac{1}{6} \pi (d_1 + d_2)^3 \kappa_2 \right] \right. \\
& \left. - \left[-\frac{1}{2} \pi d_1^2 + \frac{1}{6} \pi d_1^3 \kappa_2 \right] \right\} \quad (49)
\end{aligned}$$

$$\begin{aligned}
B_6(t) = & \frac{1}{2} k_{b3} \left\{ \left[-\frac{1}{2} \pi (d_1 + d_2 + d_3)^2 \right. \right. \\
& \left. \left. + \frac{1}{6} \pi (d_1 + d_2 + d_3)^3 \kappa_3 \right] \right. \\
& \left. - \left[-\frac{1}{2} \pi (d_1 + d_2)^2 + \frac{1}{6} \pi (d_1 + d_2)^3 \kappa_3 \right] \right\} \quad (50)
\end{aligned}$$

C. Extension Terms

The entries of $E(q)$ are given as follows

$$E_1 = k_{e1} (d_1(t) - d_1^*) \quad (51)$$

$$E_2 = k_{e2} (d_2(t) - d_2^*) \quad (52)$$

$$E_3 = k_{e3} (d_3(t) - d_3^*) \quad (53)$$

$$E_4 = 0, E_5 = 0, E_6 = 0 \quad (54)$$